Self-starting coherent mode locking in a two-section laser with identical gain and absorber media

Anton Pakhomov,[1] Mikhail Arkhipov,[1] Nikolay Rosanov,[1,2] and Rostislav Arkhipov[1,2]
[1]*St. Petersburg State University, Universitetskaya nab. 7/9, St. Petersburg 199034, Russia*
[2]*Ioffe Institute, Politekhnicheskaya str. 26, St. Petersburg 194021, Russia*

(Received 10 November 2022; accepted 6 January 2023; published 17 January 2023)

Coherent mode-locking (CML) represents a method for ultrashort pulse generation in lasers based on the self-induced transparency (SIT) phenomena, which allows us to overcome the principal limitations on the pulse duration imposed by the active medium's gain bandwidth in standard passively mode-locked lasers. So far, this regime was only studied in lasers with transition dipole moments in the absorber medium being twice larger than in the gain medium. This fact ensures that the 2π-SIT-soliton in the absorber also forms the stable π-soliton in the gain but can be barely realized in experiments. In this paper we demonstrate theoretically that the self-starting stable coherent mode-locking regime can also arise if the same medium is used both in the gain and absorber laser sections, i.e., the transition dipole moments are equal. These results are both obtained analytically using the area theorem and confirmed by the numerical solution of the Maxwell-Bloch equations. Our findings can enable new opportunities in the area of ultrafast lasers.

DOI: 10.1103/PhysRevA.107.013510

I. INTRODUCTION

The coherent light-matter interaction arises when the pulse duration is much smaller than the polarization (coherence) relaxation time T_2 in the medium [1,2]. Such interaction gives rise to the self-induced transparency (SIT) phenomena, when a light pulse can propagate in a resonant medium without changing its shape [3,4]. The coherent interaction of a pulse with a two-level resonant medium is described in terms of the so-called pulse area, defined as follows [1]:

$$\Phi(t,z) = \frac{d_{12}}{\hbar}\int_{-\infty}^{t} \mathcal{E}(t',z)dt', \tag{1}$$

where d_{12} is the transition dipole moment and $\mathcal{E}(t,z)$ is the envelope of the electric field in the pulse. Namely, a stable SIT-soliton in an absorbing two-level medium has the pulse area equal to 2π [1,4]. The pulse duration is therefore equal to one period of Rabi oscillations of the atomic inversion, i.e., at the leading edge of the pulse the medium is excited, and at the trailing edge of the pulse the medium returns back to the ground state, leading to the lossless pulse propagation.

SIT phenomena has been observed in a variety of different media so far [5–11] and has been suggested for some applications, such as the pulse compression [12]. As the most promising, however, seems the possibility of SIT- or coherent mode-locking (CML) in lasers [13], which was recently experimentally demonstrated [14,15]. Such a mode-locking mechanism relies on the formation of a SIT soliton in an active media and allows us to obtain pulses with much smaller duration as compared with the standard passive mode locking with saturable absorbers. While in standard passively mode-locked lasers based on the incoherent gain and absorber saturation the achieved pulse duration is limited by the coherence relaxation time T_2 in the active medium [16–19], by means of the coherent mode locking of the pulses much shorter in duration than T_2 are obtained, since the generated pulse interacts coherently with the laser medium [13,20–29]. In such a way pulses up to a single-cycle duration can be obtained in widely used active media [22,23,29].

In most previous studies of coherent, or self-induced transparency, mode-locking the ratio of the transition dipole moments in the gain and absorber media was equal to two: $d_{12,a} = 2d_{12,g}$ or close to this value [13,20–30]. This ratio implies that the stable 2π pulse in the absorbing medium represents at the same time the stable π pulse in the gain medium, which ensures the stable circulation of such SIT-solitons in the laser cavity. However, this criterion imposes strong limitation on the choice of the intracavity laser media. Indeed, one would then need to select gain and absorber media with close frequencies of the resonant transition and above the specific ratio of the transition dipole moments. Although such media can be engineered and some examples were even theoretically suggested in quantum cascade lasers [20,21,30], fulfilling these conditions appears a challenging problem for the experimental implementation of the coherent mode-locking regime. Therefore it looks promising to extend this regime to the simplest case of lasers with identical gain and absorber media, i.e., $d_{12,g} = d_{12,a}$.

In this paper, we demonstrate how coherent mode-locking can be realized in a two-section laser with identical media in the gain and absorber sections. We reveal the underlying pulse dynamics and find out that the stable and self-starting coherent mode locking can be reached in this case. These findings may provide a noticeable step towards the development of feasible laser sources of few-cycle pulses.

It should be emphasized that, when gain and absorber dipole moments are equal to each other, a SIT soliton cannot be formed in the absorbing medium, as we see below. In

this case, CML is based only on the π-pulse formation in both intracavity media. It is contrary to the previous studies of CML regimes, where a 2π pulse of SIT was formed in the absorber [13,20–23,26,27,29,30]. So far, CML based on π-pulse formation was studied only in a single-section laser with the coherent gain medium [28]. A detailed analysis of CML based on the π-pulse formation in a two-section laser will be presented below.

The paper is organized as follows: In Sec. II we analytically demonstrate the existence and the stability of the coherent mode locking in a two-section laser with identical and inhomogeneously broadened gain and absorber media, using the area theorem. Section III is devoted to the case of homogeneously broadened media in the gain and absorber sections and we show the stability of the CML regime through the numerical solution of Maxwell-Bloch equations. Finally, the paper summary and concluding remarks are provided in Sec. IV.

II. INHOMOGENEOUSLY BROADENED ACTIVE MEDIA

If a light pulse coherently propagates in an inhomogeneously broadened two-level absorbing (or amplifying) medium, an explicit equation can be derived for the pulse area evolution. This important result, known as the area theorem, was first obtained by McCall and Hanh and yields for the pulse area Φ [1,2,4]

$$\frac{d\Phi}{dz} = \pm\frac{\alpha_0}{2}\sin\Phi,$$
$$\alpha_0 = \frac{8\pi^2 N_0 d_{12}^2 \omega_{12} T_2^*}{\hbar c}, \tag{2}$$

where the plus sign corresponds to the amplifying medium, and the minus sign to the absorbing medium, α_0 is the gain or absorption coefficient with the concentration of two-level atoms N_0, the medium transition frequency is ω_{12}, and the width of the inhomogeneously broadened line is $1/T_2^*$. Equation (2) has the solution

$$\tan\left(\frac{\Phi}{2}\right) = \tan\left(\frac{\Phi_0}{2}\right)e^{\pm\alpha_0 z/2}, \tag{3}$$

with the initial pulse area Φ_0.

In Fig. 1 we plot a diagram showing the solution Eq. (3) both in gain and absorber media depending on the initial value of the pulse area in the range $\Phi_0 \in [0; 2\pi]$. The transition dipole moments in both media here are assumed equal. The initial value of the pulse area in Fig. 1 is assumed to be selected along the vertical axis and the depicted curves provide the respective pulse area evolution vs the coordinate z (up to an arbitrary shift along the z axis). One can see that, in the gain medium, the only stable value of the pulse area is $\Phi = \pi$ and the pulse approaches this value upon propagation for any $\Phi_0 \in (0; 2\pi)$. In contrast, in the absorber medium the state $\Phi = \pi$ is unstable, while two other stable values $\Phi = 0$ and $\Phi = 2\pi$ arise instead. If $\Phi_0 \in (0; \pi)$, the pulse propagating in the absorber approaches the pulse area $\Phi = 0$, and for $\Phi_0 \in (\pi; 2\pi)$ the pulse approaches the value of the pulse area $\Phi = 2\pi$.

We proceed now with a two-section ring-cavity laser configuration, with a gain and an absorber section placed

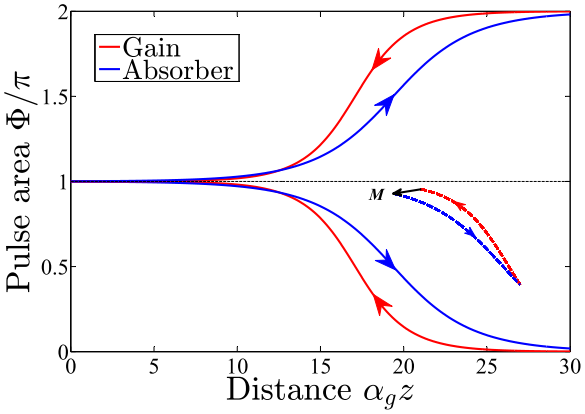

FIG. 1. Diagram showing the pulse area evolution in the gain (red curves with left arrows) and absorber media (blue curves with right arrows), $\alpha_g = 1.5\alpha_a$. Dashed lines show an example of the stable limit cycle arising in the system with $\alpha_g L_g = 6$, $L_a = 1.25L_g$, where L_g and L_a are the lengths of the gain and absorber sections respectively. Black arrow corresponds to the pulse reflection at the output mirror M with $r = 0.97$

separately inside the cavity, as sketched in Fig. 2. The output radiation is provided through the output mirror with the amplitude reflection coefficient $r = r(\omega_{12})$ at the pulse carrier frequency ω_{12}. We also assume the unidirectional lasing in the cavity, which can be ensured by placing an additional intracavity component.

As we use identical gain and absorber media, we no longer need to specify which transition dipole moment is taken in the definition Eq. (1). Let us denote the pulse area just after the gain section after n round trips inside the cavity as Φ_n. Now using Eq. (3) and the fact of identical transition dipole moments in the gain and absorber one finds the following simple expression for the value Φ_{n+1}:

$$\tan\left(\frac{\Phi_{n+1}}{2}\right) = \tan\left(\frac{r\Phi_n}{2}\right)e^{(\alpha_g L_g - \alpha_a L_a)/2}. \tag{4}$$

Here we made use of the fact strictly proven in Ref. [28] that the areas Eq. (1) of the incident and reflected pulses at the mirror are simply related through the amplitude reflection coefficient r.

In the steady-state regime we get

$$\Phi_{n+1} = \Phi_n = \Phi^*,$$

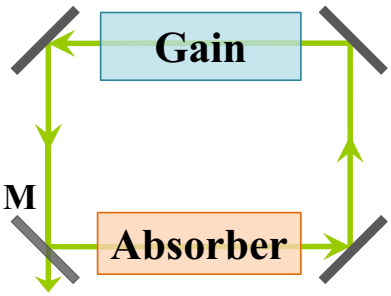

FIG. 2. The scheme of the considered two-section ring-cavity laser with the output mirror M; all other mirrors are assumed fully reflecting.

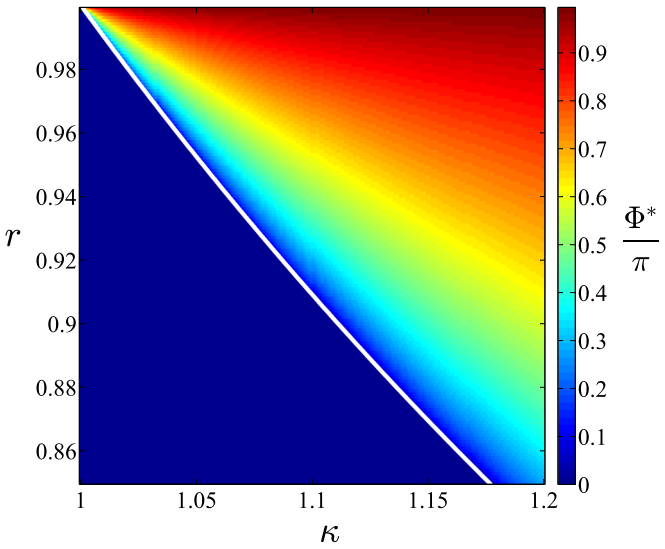

FIG. 3. The nontrivial steady-state solution Φ^* of Eq. (5) vs the mirror amplitude reflectivity r and the parameter κ from Eq. (6). to the left of the white solid line $\kappa r = 1$ only the trivial solution $\Phi^* = 0$ exists.

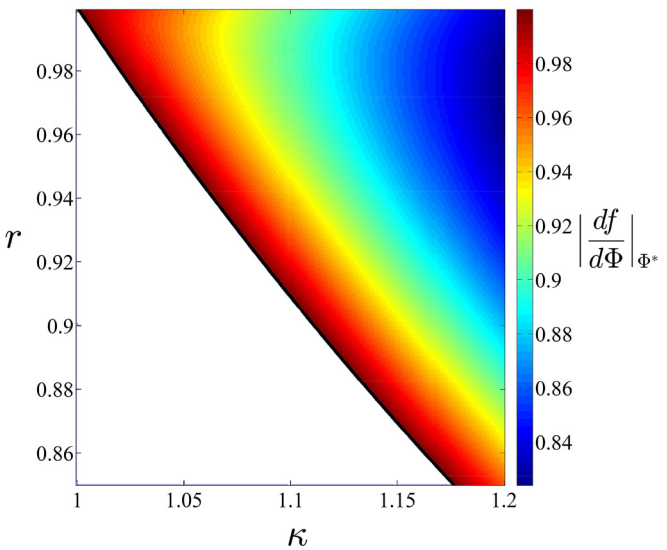

FIG. 4. The stability of the nontrivial steady-state solution Φ^* of Eq. (5), measured by the derivative (8), vs the mirror amplitude reflectivity r and the parameter κ from Eq. (6). To the left of the black solid line $\kappa r = 1$, only trivial solution $\Phi^* = 0$ exists.

so that we end up with the following equation for Φ^*:

$$\Phi^* = 2 \arctan\left[\kappa \tan\left(\frac{r\Phi^*}{2}\right)\right], \tag{5}$$

where we denote for convenience

$$\kappa = e^{(\alpha_g L_g - \alpha_a L_a)/2}. \tag{6}$$

For any values of the parameters κ and r, Eq. (5) possesses the trivial solution

$$\Phi^* = 0. \tag{7}$$

Let us check the stability of this trivial solution. We denote the function on the right-hand side of Eq. (5) as $f(\Phi)$. Then the stability of the steady state Φ^* requires that

$$\left|\frac{df}{d\Phi}\right|_{\Phi=\Phi^*} < 1, \tag{8}$$

what reduces to

$$\kappa r < \kappa^2 \sin^2\left(\frac{r\Phi^*}{2}\right) + \cos^2\left(\frac{r\Phi^*}{2}\right). \tag{9}$$

The stability criterion Eq. (9) then yields the trivial solution to be stable when

$$\kappa r < 1. \tag{10}$$

As one can easily see from Eq. (5), it has only the trivial solution Eq. (7) in the range $\Phi \in [0; \pi]$ as long as the inequality (10) is fulfilled. Inversely, if

$$\kappa r > 1,$$

a nontrivial steady state $\Phi^* \in (0; \pi]$ arises, while the trivial steady state becomes unstable. Figure 3 shows the nontrivial solution of Eq. (5) depending on the parameters κ and r. In the parameter region (10), i.e., to the left of the white solid curve in Fig. 3, one gets only the trivial steady state.

We move on now to the stability analysis of the obtained nontrivial steady state Φ^*. The stability of the nontrivial steady state can be estimated in the first approximation, if we take $\Phi^* \approx \pi$ and $r \approx 1$. Then one can reduce Eq. (9) to

$$r < \kappa,$$

which is obeyed by default since $r \leqslant 1$ always and lasing is only possible when $\kappa > 1$. In Fig. 4 we plot the calculated derivative $f'(\Phi)|_{\Phi=\Phi^*}$. One can see that the stability criterion (8) is indeed satisfied in the whole parameter region, where the nontrivial steady state exists. Therefore the obtained coherent mode-locking regime turns out unconditionally stable. It is also interesting to note that the value of the derivative in Fig. 4 decreases as one moves away from the boundary $\kappa r = 1$ meaning that our laser system reaches the stable nontrivial steady state Φ^* faster as, e.g., the value of the parameter κ gets increased for the fixed parameter r.

Hence, when a nontrivial steady state exists, one obtains the stable limit cycle for the pulse area evolution. In such stable regime of the coherent mode locking the pulse area grows from

$$F^* = 2 \arctan\left[e^{-\alpha_g L_g/2} \tan\left(\frac{\Phi^*}{2}\right)\right] \tag{11}$$

until Φ^* upon the pulse propagation in the gain section gets reduced to $r\Phi^*$ after reflection at the output mirror and finally decreases from $r\Phi^*$ to F^* upon pulse propagation in the absorber section. An example of such a stable limit cycle is demonstrated by the dashed lines in Fig. 1. The red dashed curve in Fig. 1 yields the increase of the pulse area in the gain section, the black arrow denotes the reflection at the output mirror M with the reflectivity r, and finally the blue dashed curve shows the decrease of the pulse area in the absorber section until the value (11) at the entrance of the gain

section. The limit cycle in Fig. 1 arises spontaneously from a near-zero value of the initial pulse area Φ_0 after several round trips in the cavity. One can see that, although neither a stable 0π pulse nor a stable 2π pulse is achieved in the absorber section, the arising limit cycle for the pulse area still turns out fully stable.

The obtained limit cycle exhibits some unusual features contrasting with the previous studies of the coherent mode locking. As can be seen in Fig. 3, the largest value of the pulse area in the limit cycle, namely Φ^*, in the whole available parameter range does not exceed π, but is close enough to this value. As we assume identical media in the gain and absorber sections, we therefore get close to π-pulse circulating inside the laser cavity in the coherent mode-locking regime. This behavior should be compared with the previous works on CML, where the ratio of the transition dipole moments in the gain and absorber media was equal to two: $d_{12,a} = 2d_{12,g}$ or close to this value [13,20–23,26,27,29,30]. In those papers the pulse propagated in the absorber section in SIT regime forming a stable 2π soliton.

This difference strongly alters the underlying physics of the absorber functioning in the mode-locking regime. Indeed, our approach based on the area theorem Eq. (2) has assumed that the absorber medium in Eq. (2) has noninverted population as the pulse enters the absorber section. If a stable 2π soliton is formed in the absorber, the medium makes a full Rabi flopping upon the pulse passage and returns back to the nonexcited state. However, with the π pulse inside the laser cavity the situation becomes largely different. The π pulse entering an initially nonexcited medium in the absorber section reverses the population difference, thus leaving behind already the medium with the population inversion. In order for the stable regime to be reached it is necessary that the medium relaxes back to the noninverted state before the pulse enters the absorber again after a full round trip in the cavity. It is therefore needed that the lifetime of the excited state T_1 is shorter or at least comparable to the round-trip time in the cavity.

Finally, it is important to mention the role of the coherence relaxation time T_2 for the validity of the analysis performed. The area theorem Eq. (2) is based on the assumption of the large enough value of T_2 as compared with the pulse duration, so that the coherence relaxation can be safely neglected. Basically, the main limitation on the possible pulse duration is imposed by the round-trip time of the cavity because the pulse duration is always shorter than the round-trip time (typically the pulse duration is no less than by one order of magnitude smaller than the round-trip time). Hence, we can conclude that the stability analysis performed in this section is only valid when the coherence relaxation time T_2 of the gain and absorber media is at least of the same order of magnitude as the round-trip time of the cavity. If this condition is not obeyed and the round-trip time significantly exceeds T_2, the laser can operate in the passive (incoherent) mode-locking regime with the pulse duration larger than T_2, so that the area theorem Eq. (2) does not work anymore together with the whole stability analysis above. It is also worth noting that the condition of the long-enough decoherence time T_2 has to be accompanied by the fast enough inversion relaxation time T_1, as discussed in the above paragraph.

III. HOMOGENEOUSLY BROADENED ACTIVE MEDIA

Equations (2) and (3) are derived for an inhomogeneously broadened medium, so the performed stability analysis is not directly applicable to a homogeneously broadened medium. At the same time, it seems to be of significant interest to examine whether the stable coherent mode-locking regime obtained in the previous section would also survive for homogeneously broadened active media. Hence, we aim in this section to figure out how the stability properties of the coherent mode-locking regime are exhibited in a homogeneously broadened medium. Furthermore, the analysis presented above can illustrate only the pulse area evolution in space. At the same time, to investigate deeply the pulse propagation dynamics in the gain and absorber numerical simulations are needed.

Due to the invalidity of the area theorem for homogeneously broadened media, we use the system of Maxwell-Bloch equations and study the properties of the coherent mode-locking by means of the direct numerical simulations. We solve the standard one-dimensional (1D) system of Maxwell-Bloch equations for two-level gain and absorber media by using the finite-difference time-domain (FDTD) method. As we expect long multicycle mode-locked pulses, we make use of slowly varying envelope (SVEA) and rotating-wave (RWA) approximations. Thereby the system of equations to be solved is given as [1,2]

$$\begin{aligned} \frac{\partial E}{\partial t} + c\,\frac{\partial E}{\partial z} &= -2\pi i\omega_{12}\,P_{a,g}, \\ \frac{dP_{a,g}}{dt} + \frac{P_{a,g}}{T_2} &= \frac{id_{12}^2}{\hbar}\,N_{a,g}E, \\ \frac{dN_{a,g}}{dt} + \frac{N_{a,g} - N_{0,a,g}}{T_1} &= \frac{i}{\hbar}\,P_{a,g}E, \end{aligned} \tag{12}$$

where E and $P_{a,g}$ are the slowly varying envelopes of the electric field and the polarization of the gain or absorber media, respectively, $N_{a,g} = -\Delta\rho_{a,g}\tilde{N}_{a,g}$ are the population inversion in the gain or absorber sections with the population difference $\Delta\rho = \rho_{11} - \rho_{22}$ and the density of two-level resonant centers $\tilde{N}_{a,g}$, $N_{0,a,g}$ are the equilibrium values of the population inversion, i.e., the pumping rate in gain or absorber sections. Other parameters are the transition dipole moment d_{12}, the inversion lifetime T_1, the medium coherence lifetime T_2, and the transition frequency ω_{12}. For all media parameters we deliberately skip the a, g subscripts since, as stated above, we assume in this paper identical gain and absorber media. The model equations Eq. (12) were applied to the analysis of CML regime in the ring cavity with unidirectional propagation of the electric field as in Fig. 2. One of the mirrors has the amplitude reflection coefficient r, while the other mirrors are fully reflecting.

It is important to notice that the two-level model in Eq. (12) was successfully applied for the theoretical description of the coherent pulse propagation and the self-induced transparency phenomena in different gaseous and solid-state media [1,2]. Moreover, the model (12) was also used to describe the experimentally measured features of the Rabi flopping in semiconductor media [31–33]. Finally, as several studies have demonstrated [34,35], the propagation dynamics of SIT solitons in resonant media with three or more levels well

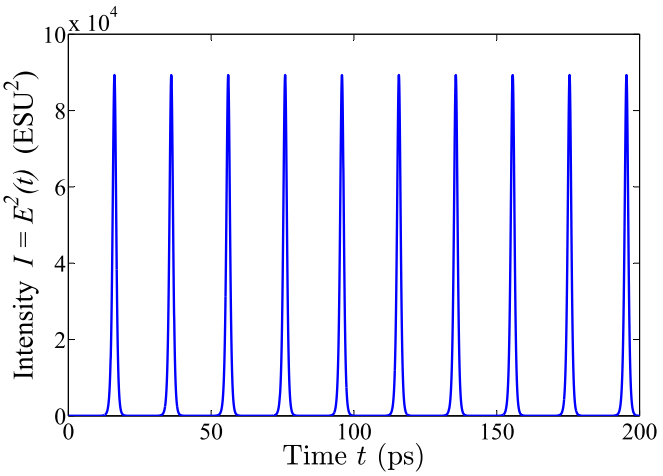

FIG. 5. The numerically obtained output pulse series from a coherently mode-locked laser. The laser parameters are listed in the text.

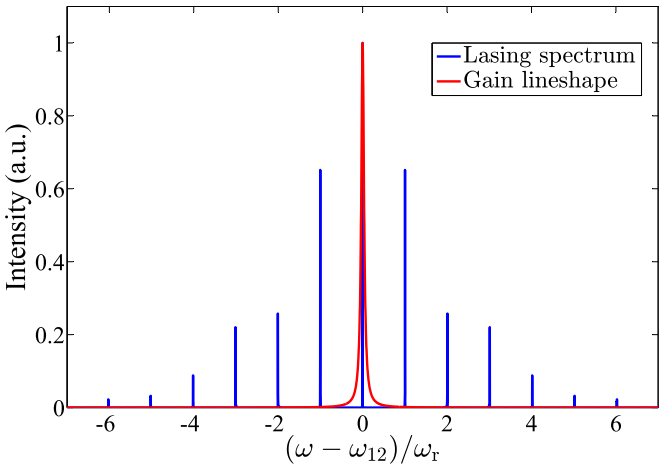

FIG. 6. The spectrum of the output pulse train from Fig. 5 (blue-colored frequency comb) together with the gain bandwidth of the gain medium (red-colored Lorentz-shaped line). ω_r is the pulse repetition angular frequency, so that $\omega_r = 2\pi/T_{rt}$ with the cavity round-trip time T_{rt}.

reproduces the one obtained with the two-level approximation. As a result, we expect the numerical simulation with the model (12) to yield quite general results, which can be well justified for a variety of different resonant media.

We take the following parameter values in the simulations: $d_{12} = 5$ D, $\omega_{12} = 2.7 \times 10^{15}$ s^{-1} ($\lambda_{12} = 700$ nm), $T_1 = 160$ ps, $T_2 = 40$ ps, $r = 0.8$, $\tilde{N}_a = \tilde{N}_g = 1.25 \times 10^{21}$ m^{-3}, $\Delta\rho_{0,g} = -1$, $\Delta\rho_{0,a} = 1$, $L_g = 0.45$ cm, $L_a = 0.15$ cm, total cavity length $L = 0.6$ cm.

As we expect our results to be applicable to many different resonant media, we do not focus here on a certain specific material but rather assume in our calculations the parameters corresponding to a "general" solid. For instance, a whole range of semiconductors and dielectrics with tunable optical parameters, like the band gap and the transition dipole moment, are available nowadays [36]. Also, present-day methods allow fabrication of arrays of different nanoparticles with tunable resonances, such as plasmonic nanostructures or semiconductor quantum dots [8,36–38]. Efficient control of the value of the relaxation time T_2 was realized, for example, in semiconductor lasers with quantum-dot active media by varying the medium's temperature with the T_2 values of several hundreds of ps achieved at low temperatures [39,40].

Numerical simulations yield self-starting stable mode-locking regime (see review [26] for more detail on self-start of CML), with the obtained time trace of the output intensity plotted in Fig. 5. This pulse series was obtained using a low-amplitude noise as the initial condition for the intracavity field, i.e., with no external seed pulses injected inside the cavity. Such property of the obtained mode locking, as the self-start, seems to be one of its most advantageous features because it can potentially allow us to greatly simplify the laser setup. The obtained pulse duration at half maximum equals 2 ps, i.e., well below the coherence relaxation time T_2, so that the pulse interaction with gain or absorber media is coherent.

Another way to confirm the coherent nature of the light-matter interaction in our setup is the lasing spectrum. In Fig. 6 we plot the spectrum of the output laser field in Fig. 5 as well as the Lorentzian gain lineshape of the active laser medium. In the case of the incoherent light-matter interaction the spectrum of the emitted field has to fall into the gain bandwidth of the active medium. The coherent light-matter interaction is inversely manifested in much broader spectrum of the laser radiation as compared with the gain bandwidth. As can be seen from Fig. 6, the obtained lasing spectrum indeed goes largely beyond the gain bandwidth, thus indicating the coherent regime of the pulse interaction with the intracavity media.

In Fig. 7 we show an instantaneous spatial distribution of the field intensity and the population difference inside the gain section as the generated pulse propagates inside. As one can see, the population difference gets almost reversed as the pulse passes through, which indicates that the pulse area is close to π. Exact calculations indeed yield the pulse area at the output of the gain section equal to 1.2π. It should also be noted that, in the considered layout, the standard passive mode

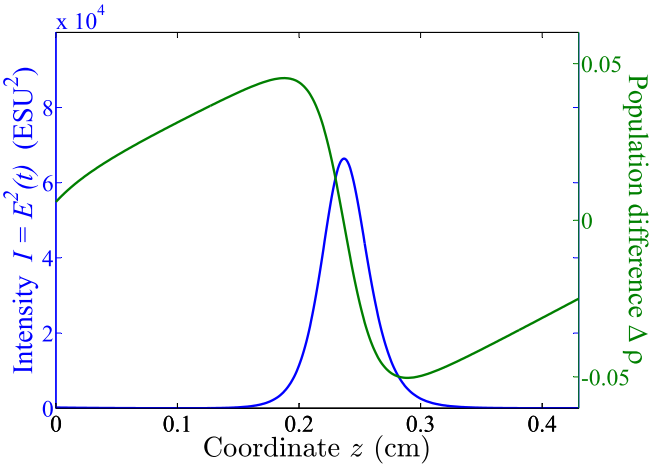

FIG. 7. The numerically obtained instantaneous spatial distribution of the field intensity [blue (dark gray) line] and the population difference in the gain section of the coherently mode-locked laser [green (light gray) line]. Parameters are the same as in Fig. 5.

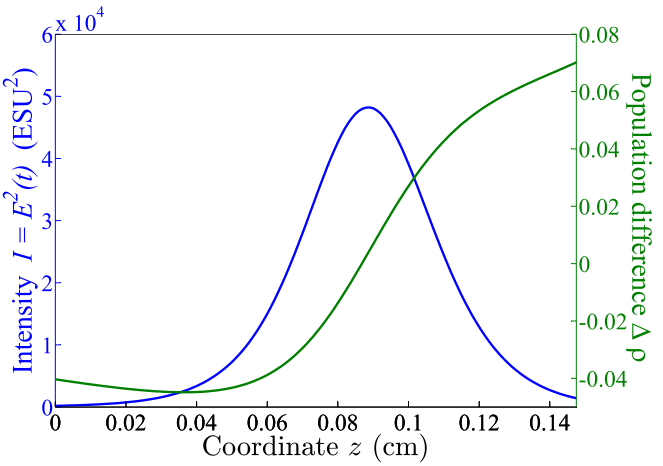

FIG. 8. The numerically obtained instantaneous spatial distribution of the field intensity [blue (dark gray) line] and the population difference in the absorber section of the coherently mode-locked laser [green (light gray) line]. Parameters are the same as in Fig. 5.

locking cannot arise, since the round-trip time $T_{\rm rt}$ in the cavity (around 20 ps) is less than the coherence relaxation time T_2, while in passively mode-locked lasers the interaction of pulses with media is incoherent, so that they produce pulses much longer in duration than the relaxation time T_2 of intracavity media. Moreover, we have also performed the numerical simulations for shorter values of T_2 down to $T_2 = 10$ ps (which is twice smaller than the round-trip time $T_{\rm rt}$) and found that the coherent mode locking is still preserved. The reason for such behavior is that the decoherence time T_2 still significantly exceeds the duration of generated mode-locked pulses (around several ps). As the result, the revealed underlying dynamics of the coherent mode-locking formation still holds.

Figure 8 demonstrates a similar instantaneous spatial distribution of the field intensity and the population difference, but inside the absorber section as the generated pulse propagates inside it. The dynamics of the population inversion appears similar to the one in Fig. 7, i.e., the population difference changes its sign upon the pulse passage with close absolute values before and after the pulse passage. Therefore we can conclude that the pulse area in the absorber section is also close to π. This finding appears to closely follow the results of the previous section for inhomogeneously broadened media, where the pulse area in the stable CML regime varied around π.

The obtained above pulse dynamics stands again in sharp contrast to the earlier described pulse evolution in the CML regime, when the transition dipole moment in the absorber medium was taken equal to the doubled transition dipole moment in the gain medium [13,20–23,26,27,29,30]. In the latter case one ended up with the stable circulation of the mode-locked pulse in the cavity, which represents the stable 2π soliton in the absorber section and at the same time the π pulse in the gain section. The absorber thus works in the self-induced transparency regime and balances the coherent pulse shortening in the gain medium.

In the case of identical gain and absorber media, while the gain medium still provides the pulse shortening and amplification with the pulse area evolving towards roughly the π pulse, the absorber section now acts in a different manner, as illustrated in Figs. 7 and 8. Namely, we do not obtain anymore the self-induced transparency with the 2π-soliton formation when the pulse leaves the absorber medium nonexcited. Instead, the mode-locked pulse in Fig. 8 reverses the medium population difference, leaving the absorber in the excited state. As the result, the relaxation dynamics in the absorber starts playing an important role in the formation of a stable coherent mode locking, similar to the aforementioned for inhomogeneously broadened active media.

It is worth to particularly address here the conditions on the value of the inversion relaxation time T_1. Figures 7 and 8 correspond to the value of T_1, which by an order of magnitude exceeds the round-trip time in the cavity $T_{\rm rt}$. In this case the population differences in the gain and absorber do not manage to completely relax back to their equilibrium values $N_{0,a,g}$, but only partially recover. As the result, in the stable coherent mode-locking regime the respective population differences in Figs. 7 and 8 do not get inverted between the values around 1 and -1, but rather attain the maximal values around 0.05–0.06. We can therefore ease the requirement on the value of T_1. Specifically, the inversion relaxation time T_1 can by orders of magnitude exceed the round-trip time in the cavity $T_{\rm rt}$ without destroying the stability properties of the coherent mode locking. The exact value of T_1 mainly determines the amplitude of the variations of the population differences in intracavity media over the round-trip time. The faster is the inversion relaxation, the more the inversion relaxes and the larger gain or absorption experiences the mode-locked pulse in the next round trip. Hence, the resulting amplitude of the obtained mode-locked pulses decreases as the value of T_1 increases. Still even much larger values of T_1 as compared with $T_{\rm rt}$ do not lead to the disappearance of the stable coherent mode-locking, but only to less intense generated pulses.

IV. CONCLUSION

We have demonstrated the possibility of the stable self-starting coherent mode locking in a two-section ring-cavity laser with identical resonant media both in the gain and absorber sections. The stability of the obtained CML regime was both proven analytically in the whole available parameter range for inhomogeneously broadened media and demonstrated numerically in the case of homogeneously broadened active media.

The underlying physics of the pulse propagation in the considered case exhibits significant differences to the previous studies of the coherent mode locking. In particular, the stabilizing role of the absorber section is now implemented in another way, i.e., instead of the formation of a stable SIT soliton with the pulse area equal to 2π, one obtains an unstable mode-locked pulse with the area close to π. Such pulse reverses the population not only in the gain medium, but also in the absorber. As the result, the fast recovery of the gain and absorption in the respective laser sections appears of crucial importance. We thus report the coherent mode-locking regime based on the π-pulse formation in two-section lasers.

As the performed analysis yields, the strongest constraint for the experimental validation of the described regimes is

the need for the long-enough coherence relaxation time T_2. Namely, the coherence relaxation time T_2 of the gain and absorber media must be at least of the same order of magnitude as the round-trip time of the cavity T_{rt}. For the cavity length of the order of millimeters, the respective values of T_2 have to be at least in the picosecond range. Such values largely exceed those for most solids at room temperatures with the relaxation times T_2 usually in the sub-ps range. Therefore certain methods to increase the coherence relaxation time must be applied. As the simplest one seems the cooling of the active media to low temperatures, where, for example, the decoherence times T_2 up to several hundred picoseconds were measured in semiconductor quantum dots [39–41].

The paper findings can provide a significant step towards the practical implementation of the CML regime. Indeed, the main limitation on the applicability of CML was the need for the specific ratio of the transition dipole moments in the gain and absorber media, namely, the transition dipole moment in the absorber medium is twice larger than in the gain medium (or at least relatively close to this value). This requirement has led to CML phenomena being an interesting but purely theoretical result, since it is hard to pick a pair of active laser media with equal resonant frequencies and such a ratio of the transition dipole moments. In this paper we have demonstrated how this principal limitation can be overcome, thus paving the way to gaining the efficiency of ultrashort pulse generation in compact lasers.

ACKNOWLEDGMENTS

The authors acknowledge support from the Foundation for the Advancement of Theoretical Physics and Mathematics "BASIS."

[1] L. Allen and J. H. Eberly, *Optical Resonance and Two-Level Atoms* (Wiley, New York, 1975).
[2] P. G. Kryukov and V. Letokhov, Sov. Phys. Usp. **12**, 641 (1970).
[3] S. L. McCall and E. L. Hahn, Phys. Rev. Lett. **18**, 908 (1967).
[4] S. L. McCall and E. L. Hahn, Phys. Rev. **183**, 457 (1969).
[5] P. Borri, W. Langbein, S. Schneider, U. Woggon, R. L. Sellin, D. Ouyang, and D. Bimberg, Phys. Rev. B **66**, 081306(R) (2002).
[6] E. Beham, A. Zrenner, F. Findeis, M. Bichler, and G. Abstreiter, Phys. Status Solidi B **238**, 366 (2003).
[7] H. Choi, V.-M. Gkortsas, L. Diehl, D. Bour, S. Corzine, J. Zhu, G. Hoefler, F. Capasso, F. Kärtner, and T. Norris, Nat. Photonics **4**, 706 (2010).
[8] A. Marini and F. Biancalana, Phys. Rev. Lett. **110**, 243901 (2013).
[9] O. Karni, A. Capua, G. Eisenstein, V. Sichkovskyi, V. Ivanov, and J. P. Reithmaier, Opt. Express **21**, 26786 (2013).
[10] M. Kolarczik, N. Owschimikow, J. Korn, B. Lingnau, Y. Kaptan, D. Bimberg, E. Schöll, K. Lüdge, and U. Woggon, Nat. Commun. **4**, 2953 (2013).
[11] S. Nandi, E. Olofsson, M. Bertolino, S. Carlström, F. Zapata, D. Busto, C. Callegari, M. Di Fraia, P. Eng-Johnsson, R. Feifel, G. Gallician, M. Gisselbrecht, S. Maclot, L. Neoričić, J. Peschel, O. Plekan, K. Prince, R. Squibb, S. Zhong, and J. Dahlström, Nature (London) **608**, 488 (2022).
[12] R. Arkhipov, M. Arkhipov, A. Demircan, U. Morgner, I. Babushkin, and N. Rosanov, Opt. Express **29**, 10134 (2021).
[13] V. V. Kozlov, Phys. Rev. A **56**, 1607 (1997).
[14] M. Arkhipov, R. Arkhipov, A. Shimko, I. Babushkin, and N. Rosanov, JETP Lett. **109**, 634 (2019).
[15] M. V. Arkhipov, A. A. Shimko, N. N. Rosanov, I. Babushkin, and R. M. Arkhipov, Phys. Rev. A **101**, 013803 (2020).
[16] U. Keller, Nature (London) **424**, 831 (2003).
[17] E. Rafailov, M. Cataluna, and W. Sibbett, Nat. Photonics **1**, 395 (2007).
[18] U. Keller, Appl. Phys. B: Lasers Opt. **100**, 15 (2010).
[19] J. C. Diels and W. Rudolph, *Ultrashort Laser Pulse Phenomena* (Elsevier, New York, 2006).
[20] C. R. Menyuk and M. A. Talukder, Phys. Rev. Lett. **102**, 023903 (2009).
[21] M. A. Talukder and C. R. Menyuk, Phys. Rev. A **79**, 063841 (2009).
[22] V. V. Kozlov, N. N. Rosanov, and S. Wabnitz, Phys. Rev. A **84**, 053810 (2011).
[23] V. V. Kozlov and N. N. Rosanov, Phys. Rev. A **87**, 043836 (2013).
[24] R. Arkhipov, M. Arkhipov, and I. Babushkin, JETP Lett. **101**, 149 (2015).
[25] R. Arkhipov, Ph.D. thesis, Humboldt-Universität zu Berlin, Mathematisch-Naturwissenschaftliche Fakultät, 2015.
[26] R. Arkhipov, M. Arkhipov, and I. Babushkin, Opt. Commun. **361**, 73 (2016).
[27] R. M. Arkhipov, M. V. Arkhipov, I. Babushkin, and N. N. Rosanov, Opt. Lett. **41**, 737 (2016).
[28] R. M. Arkhipov, A. V. Pakhomov, M. V. Arkhipov, I. V. Babushkin, and N. N. Rosanov, Sci. Rep. **11**, 1147 (2021).
[29] R. Arkhipov, M. Arkhipov, A. Pakhomov, I. Babushkin, and N. Rosanov, Phys. Rev. A **105**, 013526 (2022).
[30] O. Outafat, S. Faci, E. Richalot, S. Protat, and C. Algani, Opt. Quantum Electron. **54**, 283 (2022).
[31] O. D. Mücke, T. Tritschler, M. Wegener, U. Morgner, and F. X. Kärtner, Phys. Rev. Lett. **87**, 057401 (2001).
[32] O. D. Mücke, T. Tritschler, M. Wegener, U. Morgner, F. X. Kärtner, G. Khitrova, and H. M. Gibbs, Opt. Lett. **29**, 2160 (2004).
[33] M. Wegener, *Extreme Nonlinear Optics* (Springer, Heidelberg, 2005).
[34] N. Vysotina, N. Rosanov, and V. Semenov, JETP Lett. **83**, 279 (2006).
[35] N. V. Vysotina, N. N. Rosanov, and V. E. Semenov, Opt. Spectrosc. **106**, 713 (2009).
[36] J. Ryou, Y.-S. Kim, S. Kc, and K. Cho, Sci. Rep. **6**, 29184 (2016).
[37] P. C. Wu, T.-H. Kim, A. Suvorova, M. Giangregorio, M. Saunders, G. Bruno, A. S. Brown, and M. Losurdo, Small **7**, 751 (2011).

[38] L. Yuan, W. Hu, H. Zhang, L. Chen, J. Wang, and Q. Wang, Front. Bioeng. Biotechnol. **8**, 21 (2020).

[39] P. Borri, W. Langbein, S. Schneider, U. Woggon, R. L. Sellin, D. Ouyang, and D. Bimberg, Phys. Rev. Lett. **87**, 157401 (2001).

[40] M. Bayer and A. Forchel, Phys. Rev. B **65**, 041308(R) (2002).

[41] N. H. Bonadeo, J. Erland, D. Gammon, D. Park, D. S. Katzer, and D. G. Steel, Science **282**, 1473 (1998).